HHS Public Access

Author manuscript

Exp Eye Res. Author manuscript; available in PMC 2016 August 01.

Published in final edited form as:

Exp Eye Res. 2015 August ; 137: 103–110. doi:10.1016/j.exer.2015.06.014.

Isolation of intact astrocytes from the optic nerve head of adult mice

Hee Joo Choi, **Daniel Sun**, and **Tatjana C. Jakobs***

Department of Ophthalmology, Harvard Medical School, Massachusetts Eye and Ear Infirmary, Boston

Abstract

The astrocytes of the optic nerve head are a specialized subtype of white matter astrocytes that form the direct cellular environment of the unmyelinated ganglion cell axons. Due to their potential involvement in glaucoma, these astrocytes have become a target of research. Due to the heterogeneity of the optic nerve tissue, which also contains other cell types, in some cases it may be desirable to conduct gene expression studies on small numbers of well-characterized astrocytes or even individual cells. Here, we describe a simple method to isolate individual astrocytes. This method permits obtaining astrocytes with intact morphology from the adult mouse optic nerve and reduces contamination of the isolated astrocytes by other cell types. Individual astrocytes can be recognized by their morphology and collected under microscopic control. The whole procedure can be completed in 2-3 hours. We also discuss downstream applications like multiplex single-cell PCR and quantitative PCR (qPCR).

Keywords

astrocytes; mouse; optic nerve head; Piezo; single-cell analysis; single-cell isolation; TRPP

1. Introduction

Astrocytes are the most numerous glial cell type in the mammalian brain. Originally, their role was thought to be mainly supportive for the neurons in their vicinity. More recently, however, astrocytes have been shown to be active players in almost all CNS activity both under normal and under pathological conditions (Sofroniew and Vinters, 2010; Sun and Jakobs, 2012). In general terms, astrocytes can be subdivided into two types, the protoplasmic astrocytes that reside in the grey matter of the brain, and the fibrous astrocytes in the white matter. Both types of astrocyte respond to CNS injury of any kind by becoming reactive. This was first described as a morphological change that involves an upregulation of intermediate filaments in the cytoplasm and a hypertrophy of the cells' processes (Eng et al.,

*Correspondence to: Tatjana C. Jakobs, Schepens Eye Research Institute, 20 Staniford Street, Boston, MA 02114, Tel: 1-617-912-0205 Tatjana_Jakobs@meei.harvard.edu.

2000; Pekny and Nilsson, 2005; Sofroniew and Vinters, 2010). But reactivity also leads to profound changes in gene expression. This is well documented on the transcriptome level for protoplasmic astrocytes that lend themselves to isolation of pure populations due to their high numbers and the availability of transgenic mice with astrocyte-specific expression of GFP (Cahoy et al., 2008; Lovatt et al., 2007; Orre et al., 2014; Zamanian et al., 2012). Whether reactive changes in astrocytes are beneficial or harmful for neuronal survival or recovery after injury is an active topic of research (Karimi-Abdolrezaee and Billakanti, 2012; Sofroniew, 2005).

In glaucomatous optic neuropathy astrocyte reactivity is observed in all stages of the disease, including very early time points before obvious loss of ganglion cells has occurred in the retina (Balaratnasingam et al., 2008; Hernandez, 2000; Lye-Barthel et al., 2013). The optic nerve head, especially the region of the lamina cribrosa in primates and its glial counterpart in rodents, is thought to be the site of first injury to retinal ganglion cell axons (Howell et al., 2007; Jakobs et al., 2005; Quigley et al., 1981; Quigley et al., 1983). This has led to considerable interest in studying the cellular components of the optic nerve and their gene expression profiles in response to elevated intraocular pressure and other types of injury, such as nerve crush or transection (Howell et al., 2011a; Jakobs, 2014; Johnson et al., 2011; Johnson et al., 2007; Qu and Jakobs, 2013). However, the optic nerve contains astrocytes, microglia, NG2 expressing cells, endothelial cells, and ganglion cell axons, all of which may contribute to the total RNA extracted from the nerve for analysis. It can, therefore, be difficult to determine which cell type is responsible for the differential regulation of genes or pathways. If one wants to study pure astrocytes, it is in principle possible to establish cell cultures from the optic nerve and use them for gene expression profiling or a targeted assay of the regulation of individual genes (Hernandez et al., 2002; Miao et al., 2008; Nikolskaya et al., 2009). Unfortunately, if astrocytes are taken into culture, under most conditions they tend to change in morphology and gene expression, which complicates the analysis of biological effects (Foo et al., 2011). Though culture of pure optic nerve astrocytes remains a powerful technique, in some cases it may be preferable to work on freshly dissociated, individual cells.

Dissociated cells from various parts of the CNS in normal and pathological conditions have been used successfully to assay the expression of individual genes, multiple genes in parallel, and the construction of cDNA libraries for genetic screening or sequencing (Dulac and Axel, 1995; Jakobs et al., 2007; Janssen-Bienhold et al., 2001; Kamphuis et al., 2003; Pannicke et al., 2000; Saliba et al., 2014). A potential drawback of cell dissociation is that it can be difficult to recognize the target cells as the process involves enzymatic and mechanical disruption of the tissue which can lead to the cells losing their distinctive features. In this case, an antibody against an extracellular epitope may be used to identify the cell, if such an epitope is available (Jakobs et al., 2003). However, in many cases optimizing the dissociation protocol results in single cells with well-preserved morphology (Haseleu et al., 2013). Here we describe a method to isolate intact astrocytes from the glial lamina of the murine optic nerve and discuss downstream applications. Analysis of optic nerve head astrocytes on the single-cell level should be of interest not only in glaucoma research but also in studies that aim at understanding the biology of white matter astrocytes under normal and pathological conditions.

2. Materials and supplies

2.1. Animals

All animal were treated in accordance with the ARVO Statement for the Use of Animals in Ophthalmic and Vision Research, and all procedures were approved by the Institutional Animal Care and Use Committee at Schepens Eye Research Institute. Four mouse strains were used in this study: (1) wild-type C57BL/6 (Charles River Laboratories, Wilmington, MA). (2) A transgenic mouse line (B6.hGFAPpr-EGFP) produced by backcrossing hGFAPpr-EGFP mice that express GFP under the control of the promoter of human glial fibrillary acidic protein (GFAP) onto the C57BL/6 background. (3) B6.129P-Cx3cr1^{tm1Litt}/J mice expressing EGFP in immune cells such as microglia, monocytes, and NK cells (the Jackson laboratory, Bar Harbor, ME, strain #005582). (4) A transgenic mouse line in which astrocytes in the brain and optic nerve express red fluorescent protein. The transgenic hGFAPpr-EGFP mice on the FVB/N background (Nolte et al., 2001) were obtained from the laboratory of Helmut Kettenmann (Max Delbruck Center, Berlin, Germany). This mouse strain displays bright expression of enhanced green fluorescent protein (EGFP) in many, but not all astrocytes, thus the complete morphology of individual astrocytes can be observed directly (Sun et al., 2009, 2010; Sun et al., 2013). We crossed the hGFAPpr-EGFP mice with C57BL/6 mice for at least six generations to remove the retinal degeneration mutation in the FVB/N-derived transgenic mice. To generate mice that express a red fluorescent protein in astrocytes under the control of the GFAP promoter, we crossed B6.Cg-Tg(Gfap-cre)73.12Mvs/J with the reporter strain B6;129S6-Gt(ROSA)26Sor$^{tm9(CAG-tdTomato)Hze}$/J (both from the Jackson laboratory, Bar Harbor, ME, strain numbers 012886 and 007905, respectively). This strain was used as an additional method to ensure that the isolated cells were astrocytes. Mice were housed under a 12 h light/dark cycle with free access to food and water.

2.2. Reagents

Reagents used in cell dissociation and single cell collection were: 10× phosphate-buffered saline (PBS; USB, Cleveland, OH), Ca^{2+}/Mg^{2+} free Hank's balanced salt solution (HBSS, Lonza, Walkersville, MD), Papain (Worthington Cat No. 3126, Lakewood, NJ), and Normal horse serum (Jackson Immuno Research, West Grove, PA). DNAse (Cat No. D-5025, 15,000 U/ml), BSA (Cat No. A-2153), and L-Cysteine (Cat No. C-1276) were purchased from Sigma-Aldrich (St. Louis, MO). For single-cell reverse-transcription polymerase chain reaction (RT-PCR) in 3.3 the Access RT-PCR system (Promega Cat No. A1250, Madison, WI) was used for reverse transcription and the first round of PCR, and the AmpliTaq Gold® DNA Polymerase (Applied Biosystems Cat No. 4311814, Foster City, CA) was used for the second round of PCR. For qPCR in 3.4 the Arcturus Pico Pure RNA isolation kit (Applied Biosystems, Cat No. 12204-01) was used to extract total RNA from 12 astrocytes and the RNA was transcribed and amplified using an Ovation qPCR system kit (NuGen, Cat No. 2210-24, San Carlos, CA).

2.3. Equipment

Transverse sections of B6.hGFAPpr-EGFP and B6.129P-Cx3cr1^{tm1Litt}/J mice were made on a TPI Vibratome 1000 (Technical Products International, Inc., St. Louis, MO), and the

images were taken using a Leica SP5 confocal microscope (Leica Microsystems, Buffalo Grove, IL).

Collecting single astrocytes was performed using glass micropipettes (World Precision Instruments Cat No. TW150-4) attached to manual linear stages (Newport M-423, Franklin, MA) under a Zeiss Axiovert 200 with Hoffman optics (Fig. 1A). The glass micropipettes were pulled with a two-stage puller (Narishige PP-83, Tokyo, Japan) to produce ~20 μm tips before use.

Gold Seal microscope slides were used to hold the cell suspension and the washing buffer (Gold Seal Fluorescent Antibody Micro Slides with 2 etched rings, Gold Seal Products Cat No. 3032, Portsmouth, NH).

Single-cell RT-PCR in 3.3 and qPCR in 3.4 were performed in the GeneAmp PCR System 9700 (Applied Biosystems) and in the StepOnePlus qPCR thermocycler (Applied Biosystems), respectively.

3. Detailed methods

3.1. Isolation of single astrocytes from the optic nerve head

Before the start of the experiment, the enzymatic cell dissociation solution is freshly prepared by adding 9 μl papain suspension (the concentration of papain is ~35 mg protein per ml, with the exact concentration dependent on the lot) and 2.5 μl L-cystein solution (10 mg/ml in HBSS) to 500 μl HBSS. The cell dissociation solution is incubated at 37°C for 15 min to activate the papain. During that time, the mouse is euthanized with CO_2, and the mouse eyes are pulled out using a pair of curved forceps and placed in pre-chilled PBS. The extraocular muscles, meningeal sheath, cornea, lens, and sclera are removed, and then the optic nerve head is dissected from the retina and the myelinated region of the optic nerve. Due to the small amount of tissue, two optic nerve heads are used for cell dissociation. The optic nerve heads are transferred into the papain solution and incubated for 15-25 min. The incubation time should be adjusted depending on the age of mice (older mice generally needing longer incubation times). After enzymatic treatment, digested optic nerve heads are centrifuged at 2000 rpm for 5 min at room temperature to remove the papain solution. The optic nerve heads are resuspended in 200 μl HBSS with 10% normal horse serum to stop the enzymatic reaction and mechanically dissociated by gentle trituration 3-5 times using a heat-polished Pasteur pipette (the lumen diameter at the tip of the pipet should be approximately 300 μm). The cell suspension and undissociated tissue are centrifuged again at 2000 rpm for 5 min at room temperature and resuspended in 200 μl HBSS containing 10% horse serum and 60 U/ml DNase to remove extracellular DNA. Lastly, the undissociated tissue is triturated with a series of heat-polished Pasteur pipettes with progressively smaller openings (~300 μm to 100 μm) until it is completely dissociated. The resulting cell suspension is kept on ice and used within an hour. (The cell suspension still contains the DNAse, but it does not interfere with downstream applications.)

Astrocytes dissociated from the optic nerve head have thick, elongated cell bodies and 6-8 primary processes that extend in all directions (Fig. 1E-F and Fig. 2; two astrocytes are

shown in Fig. 1 E2). The astrocyte in Fig. 1 E2 had an unbranched process extending a long distance (arrowheads), consistent with that the processes of optic nerve head astrocytes could span most of the diameter of the optic nerve (Sun et al., 2009). These morphological properties are quite similar to the morphology of optic nerve head astrocytes in vivo that was observed from transverse sections of the optic nerve head of B6.hGFAPpr-EGFP mice, in which astrocytes express EGFP (Fig. 1C), as well as that was described in previous studies (Sun et al., 2009, 2010; Sun et al., 2013). For comparison, a microglial cell from a B6.129P-Cx3cr1^{tm1Litt}/J mouse was imaged in the same way (Fig. 1D). Microglia are much smaller than astrocytes, and their processes are more delicate.

Astrocytes are the most abundant cell type in the optic nerve head, occupying up to 50% of the tissue volume (Skoff et al., 1986). However, the optic nerve head also contains several other components such as microglia, blood vessels, and ganglion cell axons. As an additional confirmation that the cells obtained with our isolation method are indeed astrocytes, we use a transgenic mouse strain that expresses red fluorescent protein in astrocytes. Cells dissociated from the optic nerve head of the GFAP-Cre × tdTomato mice are identified as individual astrocytes by tdTomato labeling (Fig. 2).

3.2. Single astrocyte collection

About 50 μl of the cell suspension are pipetted into one of the rings on a Gold Seal slide (Fig. 1B #1), and the same volume of washing buffer (1× PBS containing 2% BSA) is pipetted into the other ring (Fig. 1B #2). The cells are allowed to settle down on the slide (about 3 minutes). Then individual, isolated cells are visualized and aspirated into the micropipette (Figs. 1 F and G). The cell is transferred to the washing buffer and expelled from the pipette. Then the cell is aspirated again with a fresh micropipette and transferred into a thin-wall PCR tube that contained 5 μl of RT-PCR mix (Fig. 1B #3, 1× Reaction Buffer from the Access RT-PCR kit and a mix of all primer pairs to be tested, including the internal controls, at 1-2 μM each primer). The tube is centrifuged briefly and immediately put on dry ice until further use.

3.3. Downstream application 1: single-cell RT-PCR

The tubes containing single astrocytes are thawed and heated to 65 °C for 1.5 minutes and 37 °C for 2 minutes to facilitate primer annealing. The Access RT-PCR kit is used for reverse transcription and the first round of PCR. The concentration of Mg^{2+}, dNTPs, and the enzymes (AMV reverse transcriptase and Tfl polymerase) are used as recommended by the supplier. The reaction mixture is incubated for 50 minutes at 48 °C for reverse transcription. The first round PCR is performed in the same tube as per the manufacturer's instructions; however we found that reducing the numbers of cycles for the first round PCR to 18-19 reduces non-specific amplification in the second round. We generally do not detect bands on an agarose gel after the first round.

The second round PCR reactions are carried out individually for each primer pair (Fig. 3A). We routinely use nested primer pairs (at 0.6 μM each, Appendix 1) for the second round as this increases specificity. Fig. 3B shows two examples of single-cell RT-PCR. In this case the cells were assayed for seven genes: the transient receptor potential channels P1 and P2

(TRPP1 and TRPP2), the Piezo channels 1 and 2, and several control genes, namely GFAP as a positive control for astrocytes, myelin basic protein (MBP) to rule out contamination by oligodendrocytes, and CD45 as a negative control for microglia and macrophages (Spandidos et al., 2010). However, we have successfully tested over 30 genes simultaneously in a single cell. The test genes (TRPP1, TRPP2. Piezo 1, and Piezo 2) were chosen because their transcripts are expressed in whole optic nerve tissue at a low level (Choi, under review) and we wanted to verify that it is possible to detect even relatively rare mRNA species in single astrocytes.

3.4. Downstream application 2: qPCR from single astrocytes or small numbers of astrocytes

It is in principle possible to perform qPCR from single cells, and our protocol could easily be modified to perform qPCR as the second round PCR. However, it should be noted that the variability of qPCR experiments in single cells is considerable and cannot completely be eliminated by optimizing the reaction conditions for each step (Reiter et al., 2011). Rather, the variability reflects the "stochastic" nature of gene expression over time and the heterogeneity even amongst neighboring cells (Cai et al., 2006; Junker and van Oudenaarden, 2014). If one wanted to compare different conditions (in our case the astrocytes from the contralateral eye versus astrocytes that have been subjected to a crush injury) it would be necessary to probe many individual cells. We therefore pool several cells for reverse transcription followed by qPCR.

The astrocytes are collected as described in 3.2, however 12 cells are pooled together in 5 μl PBS in the same tube. Total RNA is extracted using the Arcturus Pico Pure RNA isolation kit and the RNA is transcribed and amplified using an Ovation qPCR system kit. As an example, we present the results of qPCR from 12 astrocytes from the optic nerve head 1 day after a crush injury compared to 12 astrocytes from the uninjured contralateral eye. We tested the expression levels of the genes for the intermediate filaments GFAP and vimentin in four biological replicates for each condition (Fig. 4, Appendix 2). These two genes were chosen to validate the method because the changes in gene expression for both were known from prior experiments. GFAP is significantly (though not dramatically) up-regulated on the protein level after optic nerve crush (Sun et al., 2013). Both GFAP and vimentin are not significantly differentially regulated in whole optic nerve head tissue after injury when assayed by microarray (Qu and Jakobs, 2013), and are up-regulated slightly (~1.25-fold) when assayed by qPCR. In earlier studies we found the most pronounced up- or down-regulation of gene expression for the majority of genes is observed shortly after injury (Qu and Jakobs, 2013), so one day after nerve crush was chosen as the time point for astrocyte collection in this study. In order to analyze qPCR data we obtained averaged Ct data of three technical replicates for each of four biological samples and performed the $2^{-\Delta\Delta CT}$ calculation to determine the relative changes in gene expression. Both genes were moderately up-regulated one day after injury (~2.7-fold) in these purified samples of astrocytes as compared to the same number of cells from the uninjured contralateral eye (Fig. 4 F). GFAP and vimentin are considered typical "reactivity markers" for astrocytes in other parts of the CNS and they are robustly induced in pathological conditions such as cerebral ischemia (Zamanian et al., 2012). In the optic nerve, however, intermediate filament

genes are up-regulated only moderately after injury, a finding that also holds true for glaucoma (Howell et al., 2011a; Howell et al., 2011b). The likely reason is that in contrast to most other regions of the CNS, the optic nerve head already has a very high baseline expression of GFAP and vimentin even under normal conditions. Oaz1 (ornithine decarboxylase antizyme 1) was used as an internal standard because we found in preliminary experiments that the more common "housekeeping" genes GAPDH, β-actin, and S18 were themselves regulated by nerve injury (data not shown).

3.5. Accessory methods used in this study

Optic nerve crush was performed approximately 200 μm behind the globe according to published methods (Qu and Jakobs, 2013; Sun et al., 2010). Confocal image stacks were taken through individual astrocytes and microglia in 100 μm thick agarose sections of optic nerve heads from B6.hGFAPpr-EGFP mice (astrocytes) and B6.129P-Cx3cr1^{tm1Litt}/J mice (microglia). Images are acquired on a Leica SP5 confocal microscope with an X63/1.3 glycerol immersion lens. All images are maximum intensity projections of a Z-stack taken at 0.5 μm step size.

4. Potential pitfalls and troubleshooting

It is easiest to isolate single cells if they express a fluorescent marker such as GFP or RFP (Fig. 1 and 2). One of the major advantages of using mice in glaucoma research is the availability of transgenic strains, such as knock-out strains or strains that harbor particular mutations in disease-relevant genes. Most of these strains, however, do not also express a fluorescent marker in astrocytes. It is of course possible to cross a knock-out stain with a GFP-expressing strain, but it can be time-consuming to generate enough experimental animals, especially if the mice need to be homozygous for the deleted gene to show a phenotype. An additional difficulty can arise when the transgenic strain of interest and the GFP-expressing strain are not on the same genetic background. Altering the genetic background can lead to additional variability in gene expression studies (Sandberg et al., 2000), or to unexpected phenotypes – the relative resistance of C57BL/6 mice to glaucoma in the presence of mutations in the *Gpnmb* and *Trp*1 genes being a well-known example (Anderson et al., 2006). Therefore, a more versatile method of isolating cells that does not rely on the expression of fluorescent markers would be welcome. This depends on the ability to recognize astrocytes by their morphology even after dissociation. Most of the other components of the optic nerve head either do not survive the dissociation procedure intact (such as axons) or are morphologically very distinct from astrocytes (such as endothelial cells). The only cells that might be mistaken for astrocytes are microglial cells or macrophages, which are present in the optic nerve head. However, microglia/macrophages are much smaller (see Figs. 1C and 1D). Their processes are also more delicate and usually break off during the dissociation procedure so that microglia/macrophages present as small, slightly oval cell bodies. If one wants to collect single microglia/macrophages, it is advisable to use a GFP-expressing strain (e.g. B6.129P-Cx3cr1^{tm1Litt}/J).

The yield of cells with good morphology is dependent on the age of the animal. If at all possible, young adults (1-2 months) should be used. We have collected astrocytes from older (8 months) animals, but success is inconsistent (some preparations do not contain any

recognizable cells) and the yield is low. In some mouse models, such as DBA/2J, the glaucomatous degeneration takes many months to develop, so that animals at 6 – 8 months generally show only moderate, if any, ganglion cell loss in the retina (Libby et al., 2005), though there are morphological and genetic changes in the optic nerve head (Howell et al., 2011a; Lye-Barthel et al., 2013). Given the difficulty of isolating astrocytes from older animals, only the early stages of glaucoma could be studied by this method.

In general, papain concentration, incubation time, and the amount of trituration should be kept to the minimum that is just sufficient to break up all macroscopically visible chunks of tissue (small clusters of undissociated cells that are visible under the microscope are common and do not interfere with cell collection).

Occasionally, the astrocytes stick to the interior wall of the micropipette and are not easily expelled into the reaction tube. This usually occurs about one hour after the dissociation procedure and probably indicates that the cells are no longer viable. It is therefore recommended to use a preparation for no longer than an hour. If it is a pervasive problem that occurs even with fresh cells, the glass micropipettes should be silanized after pulling. For the silane coating, the pipette tips are first dipped in a 5% silane (Sigma-Aldrich, Cat No. 440272) in toluene solution, then the excess is removed by applying positive pressure through a syringe. The micropipettes are completely dried at room temperature overnight before use.

Though a single cell may contain fewer than 10 molecules of a low-abundance mRNA, the detection even of these rare transcripts by RT-PCR is not difficult per se. We found that in virtually all cases where we transferred the cell successfully to the PCR tube, amplicons were detected after the second round of PCR. This underscores that it is desirable to do every step, including the final transfer, under microscopic control; and an inverted microscope with long working-distance objectives should be used. By far the most common problem is a contamination of the PCR reaction. The dissociation procedure leads to the fragmentation of some of the cells in the optic nerve and cell debris or RNA that has spilled into the medium from lysing cells can be inadvertently collected together with the astrocyte. To prevent this, we found it useful to wash the cell once in fresh medium and aspirate it again with a new micropipette before transferring it to the tube. This does reduce the incidence of contamination, however, in every case positive and negative internal controls should be performed. We routinely test for transcripts of MBP and CD45 to rule out contamination by oligodendrocyte and microglia mRNA, and exclude cells that test positive for either of these genes from further analysis.

Supplementary Material

Refer to Web version on PubMed Central for supplementary material.

Acknowledgements

This work was supported by NIH grants EY019703 and EY022092, and the Lefler Foundation from Harvard Medical School. The authors thank Meredith Gregory-Ksander, PhD, for critically reading the manuscript.

References

Anderson MG, Libby RT, Mao M, Cosma IM, Wilson LA, Smith RS, John SW. Genetic context determines susceptibility to intraocular pressure elevation in a mouse pigmentary glaucoma. BMC Biol. 2006; 4:20. [PubMed: 16827931]

Balaratnasingam C, Morgan WH, Bass L, Ye L, McKnight C, Cringle SJ, Yu DY. Elevated pressure induced astrocyte damage in the optic nerve. Brain Res. 2008; 1244:142–154. [PubMed: 18848926]

Cahoy JD, Emery B, Kaushal A, Foo LC, Zamanian JL, Christopherson KS, Xing Y, Lubischer JL, Krieg PA, Krupenko SA, Thompson WJ, Barres BA. A transcriptome database for astrocytes, neurons, and oligodendrocytes: a new resource for understanding brain development and function. J Neurosci. 2008; 28:264–278. [PubMed: 18171944]

Cai L, Friedman N, Xie XS. Stochastic protein expression in individual cells at the single molecule level. Nature. 2006; 440:358–362. [PubMed: 16541077]

Dulac C, Axel R. A novel family of genes encoding putative pheromone receptors in mammals. Cell. 1995; 83:195–206. [PubMed: 7585937]

Eng LF, Ghirnikar RS, Lee YL. Glial fibrillary acidic protein: GFAP-thirty-one years (1969-2000). Neurochem Res. 2000; 25:1439–1451. [PubMed: 11059815]

Foo LC, Allen NJ, Bushong EA, Ventura PB, Chung WS, Zhou L, Cahoy JD, Daneman R, Zong H, Ellisman MH, Barres BA. Development of a method for the purification and culture of rodent astrocytes. Neuron. 2011; 71:799–811. [PubMed: 21903074]

Haseleu J, Anlauf E, Blaess S, Endl E, Derouiche A. Studying subcellular detail in fixed astrocytes: dissociation of morphologically intact glial cells (DIMIGs). Front Cell Neurosci. 2013; 7:54. [PubMed: 23653590]

Hernandez MR. The optic nerve head in glaucoma: role of astrocytes in tissue remodeling. Prog Retin Eye Res. 2000; 19:297–321. [PubMed: 10749379]

Hernandez MR, Agapova OA, Yang P, Salvador-Silva M, Ricard CS, Aoi S. Differential gene expression in astrocytes from human normal and glaucomatous optic nerve head analyzed by cDNA microarray. Glia. 2002; 38:45–64. [PubMed: 11921203]

Howell GR, Libby RT, Jakobs TC, Smith RS, Phalan FC, Barter JW, Barbay JM, Marchant JK, Mahesh N, Porciatti V, Whitmore AV, Masland RH, John SW. Axons of retinal ganglion cells are insulted in the optic nerve early in DBA/2J glaucoma. J Cell Biol. 2007; 179:1523–1537. [PubMed: 18158332]

Howell GR, Macalinao DG, Sousa GL, Walden M, Soto I, Kneeland SC, Barbay JM, King BL, Marchant JK, Hibbs M, Stevens B, Barres BA, Clark AF, Libby RT, John SW. Molecular clustering identifies complement and endothelin induction as early events in a mouse model of glaucoma. J Clin Invest. 2011a; 121:1429–1444. [PubMed: 21383504]

Howell GR, Walton DO, King BL, Libby RT, John SW. Datgan, a reusable software system for facile interrogation and visualization of complex transcription profiling data. BMC Genomics. 2011b; 12:429. [PubMed: 21864367]

Jakobs TC. Differential gene expression in glaucoma. Cold Spring Harb Perspect Med. 2014; 4:a020636. [PubMed: 24985133]

Jakobs TC, Ben Y, Masland RH. CD15 immunoreactive amacrine cells in the mouse retina. J Comp Neurol. 2003; 465:361–371. [PubMed: 12966561]

Jakobs TC, Ben Y, Masland RH. Expression of mRNA for glutamate receptor subunits distinguishes the major classes of retinal neurons, but is less specific for individual cell types. Mol Vis. 2007; 13:933–948. [PubMed: 17653033]

Jakobs TC, Libby RT, Ben Y, John SW, Masland RH. Retinal ganglion cell degeneration is topological but not cell type specific in DBA/2J mice. J Cell Biol. 2005; 171:313–325. [PubMed: 16247030]

Janssen-Bienhold U, Schultz K, Gellhaus A, Schmidt P, Ammermuller J, Weiler R. Identification and localization of connexin26 within the photoreceptor-horizontal cell synaptic complex. Vis Neurosci. 2001; 18:169–178. [PubMed: 11417791]

Johnson EC, Doser TA, Cepurna WO, Dyck JA, Jia L, Guo Y, Lambert WS, Morrison JC. Cell proliferation and interleukin-6-type cytokine signaling are implicated by gene expression

responses in early optic nerve head injury in rat glaucoma. Invest Ophthalmol Vis Sci. 2011; 52:504–518. [PubMed: 20847120]

Johnson EC, Jia L, Cepurna WO, Doser TA, Morrison JC. Global changes in optic nerve head gene expression after exposure to elevated intraocular pressure in a rat glaucoma model. Invest Ophthalmol Vis Sci. 2007; 48:3161–3177. [PubMed: 17591886]

Junker JP, van Oudenaarden A. Every cell is special: genome-wide studies add a new dimension to single-cell biology. Cell. 2014; 157:8–11. [PubMed: 24679522]

Kamphuis W, Dijk F, O'Brien BJ. Gene expression of AMPA-type glutamate receptor subunits in rod-type ON bipolar cells of rat retina. Eur J Neurosci. 2003; 18:1085–1092. [PubMed: 12956708]

Karimi-Abdolrezaee S, Billakanti R. Reactive astrogliosis after spinal cord injury-beneficial and detrimental effects. Mol Neurobiol. 2012; 46:251–264. [PubMed: 22684804]

Libby RT, Anderson MG, Pang IH, Robinson ZH, Savinova OV, Cosma IM, Snow A, Wilson LA, Smith RS, Clark AF, John SW. Inherited glaucoma in DBA/2J mice: pertinent disease features for studying the neurodegeneration. Vis Neurosci. 2005; 22:637–648. [PubMed: 16332275]

Lovatt D, Sonnewald U, Waagepetersen HS, Schousboe A, He W, Lin JH, Han X, Takano T, Wang S, Sim FJ, Goldman SA, Nedergaard M. The transcriptome and metabolic gene signature of protoplasmic astrocytes in the adult murine cortex. J Neurosci. 2007; 27:12255–12266. [PubMed: 17989291]

Lye-Barthel M, Sun D, Jakobs TC. Morphology of astrocytes in a glaucomatous optic nerve. Invest Ophthalmol Vis Sci. 2013; 54:909–917. [PubMed: 23322566]

Miao H, Chen L, Riordan SM, Li W, Juarez S, Crabb AM, Lukas TJ, Du P, Lin SM, Wise A, Agapova OA, Yang P, Gu CC, Hernandez MR. Gene expression and functional studies of the optic nerve head astrocyte transcriptome from normal African Americans and Caucasian Americans donors. PLoS One. 2008; 3:e2847. [PubMed: 18716680]

Nikolskaya T, Nikolsky Y, Serebryiskaya T, Zvereva S, Sviridov E, Dezso Z, Rahkmatulin E, Brennan RJ, Yankovsky N, Bhattacharya SK, Agapova O, Hernandez MR, Shestopalov VI. Network analysis of human glaucomatous optic nerve head astrocytes. BMC Med Genomics. 2009; 2:24. [PubMed: 19426536]

Nolte C, Matyash M, Pivneva T, Schipke CG, Ohlemeyer C, Hanisch UK, Kirchhoff F, Kettenmann H. GFAP promoter-controlled EGFP-expressing transgenic mice: a tool to visualize astrocytes and astrogliosis in living brain tissue. Glia. 2001; 33:72–86. [PubMed: 11169793]

Orre M, Kamphuis W, Osborn LM, Melief J, Kooijman L, Huitinga I, Klooster J, Bossers K, Hol EM. Acute isolation and transcriptome characterization of cortical astrocytes and microglia from young and aged mice. Neurobiol Aging. 2014; 35:1–14. [PubMed: 23954174]

Pannicke T, Fischer W, Biedermann B, Schadlich H, Grosche J, Faude F, Wiedemann P, Allgaier C, Illes P, Burnstock G, Reichenbach A. P2X7 receptors in Muller glial cells from the human retina. J Neurosci. 2000; 20:5965–5972. [PubMed: 10934244]

Pekny M, Nilsson M. Astrocyte activation and reactive gliosis. Glia. 2005; 50:427–434. [PubMed: 15846805]

Qu J, Jakobs TC. The Time Course of Gene Expression during Reactive Gliosis in the Optic Nerve. PLoS One. 2013; 8:e67094. [PubMed: 23826199]

Quigley HA, Addicks EM, Green WR, Maumenee AE. Optic nerve damage in human glaucoma. II. The site of injury and susceptibility to damage. Arch Ophthalmol. 1981; 99:635–649. [PubMed: 6164357]

Quigley HA, Hohman RM, Addicks EM, Massof RW, Green WR. Morphologic changes in the lamina cribrosa correlated with neural loss in open-angle glaucoma. Am J Ophthalmol. 1983; 95:673–691. [PubMed: 6846459]

Reiter M, Kirchner B, Muller H, Holzhauer C, Mann W, Pfaffl MW. Quantification noise in single cell experiments. Nucleic Acids Res. 2011; 39:e124. [PubMed: 21745823]

Saliba AE, Westermann AJ, Gorski SA, Vogel J. Single-cell RNA-seq: advances and future challenges. Nucleic Acids Res. 2014; 42:8845–8860. [PubMed: 25053837]

Sandberg R, Yasuda R, Pankratz DG, Carter TA, Del Rio JA, Wodicka L, Mayford M, Lockhart DJ, Barlow C. Regional and strain-specific gene expression mapping in the adult mouse brain. Proc Natl Acad Sci U S A. 2000; 97:11038–11043. [PubMed: 11005875]

Skoff, R.; Knapp, PE.; Bartlett, WP. Astrocyte diversity in the optic nerve: a cytoarchitectural study. In: Fedoroff, S.; Vernadakis, A., editors. Astrocytes. Academic Press; New York: 1986. p. 269-291.

Sofroniew MV. Reactive astrocytes in neural repair and protection. Neuroscientist. 2005; 11:400–407. [PubMed: 16151042]

Sofroniew MV, Vinters HV. Astrocytes: biology and pathology. Acta Neuropathol. 2010; 119:7–35. [PubMed: 20012068]

Spandidos A, Wang X, Wang H, Seed B. PrimerBank: a resource of human and mouse PCR primer pairs for gene expression detection and quantification. Nucleic Acids Res. 2010; 38:D792–799. [PubMed: 19906719]

Sun D, Jakobs TC. Structural remodeling of astrocytes in the injured CNS. Neuroscientist. 2012; 18:567–588. [PubMed: 21982954]

Sun D, Lye-Barthel M, Masland RH, Jakobs TC. The morphology and spatial arrangement of astrocytes in the optic nerve head of the mouse. J Comp Neurol. 2009; 516:1–19. [PubMed: 19562764]

Sun D, Lye-Barthel M, Masland RH, Jakobs TC. Structural remodeling of fibrous astrocytes after axonal injury. J Neurosci. 2010; 30:14008–14019. [PubMed: 20962222]

Sun D, Qu J, Jakobs TC. Reversible reactivity by optic nerve astrocytes. Glia. 2013

Zamanian JL, Xu L, Foo LC, Nouri N, Zhou L, Giffard RG, Barres BA. Genomic analysis of reactive astrogliosis. J Neurosci. 2012; 32:6391–6410. [PubMed: 22553043]

Highlights

- It is often difficult to isolate specific cells from a complex tissue for analysis.
- We describe a method to dissociate ONH astrocytes with intact morphology.
- A detailed method for collecting single cells is described.
- We discuss downstream applications for analysis of single astrocytes.

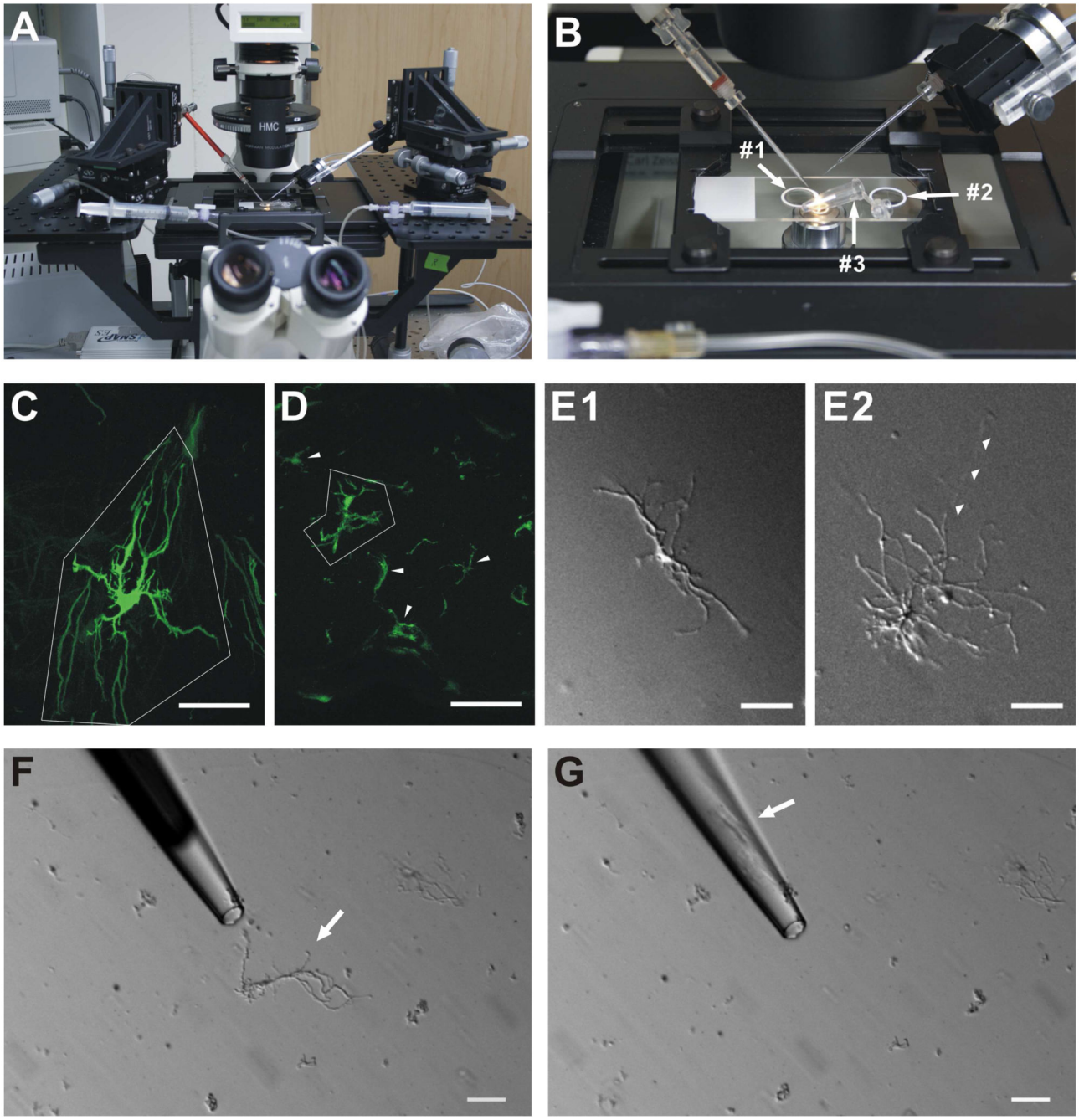

Fig. 1.

Acute dissociation of astrocytes from the optic nerve head. **A.** Experimental setup on a Zeiss Axiovert 200 equipped with two micromanipulators to direct the glass pipettes. The negative and positive pressures to aspirate and expel the cell are applied by connecting the micropipettes to 5 ml Luer lock syringes. **B.** Gold Seal slide with two rings to hold the cell suspension (#1) and the washing buffer (#2). The rings are far enough apart that a thin-wall 0.2 ml PCR tube can be placed in the middle. Five μl of reaction buffer containing all first-round primers are placed near the mouth of the tube (#3). **C.** Astrocyte morphology in a

transverse agarose section through the optic nerve head of a B6.hGFAPpr-EGFP mouse (green, irregular polygon). **D.** Microglia/macrophage in a transverse agarose section through the optic nerve head of a B6.129P-Cx3cr1^{tm1Litt}/J mouse for comparison (green, irregular polygon). Cell bodies or processes of out-of-focus microglia are indicated by arrowheads. **E1-E2.** Dissociated cells show the unique morphology of optic nerve head astrocytes with elongated cell bodies and long primary processes. Some primary processes extend for more than 150 μm (**E2**, arrowheads). **F-G.** Collecting a single astrocyte (arrows) with a glass micropipette. All scale bars: 40 μm.

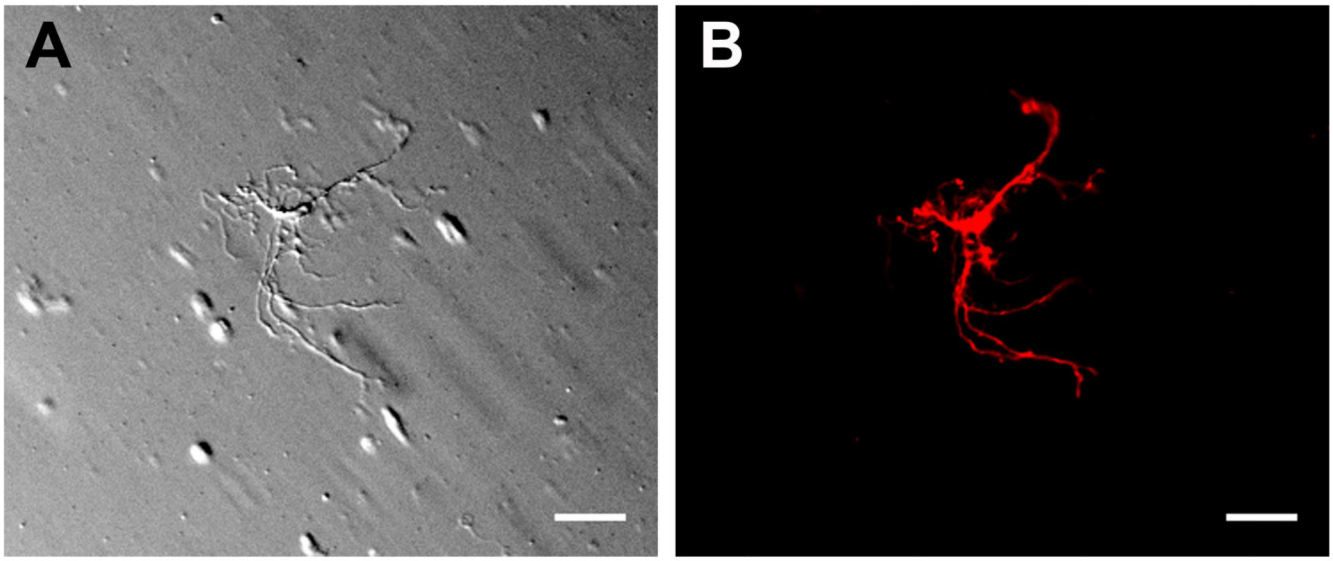

Fig. 2.

Use of GFAP-Cre × tdTomato mice to confirm that the isolated cells are astrocytes. **A.** Hoffman modulation contrast. **B.** Same cell under red fluorescence for tdTomato expression. Scale bar: 40 μm.

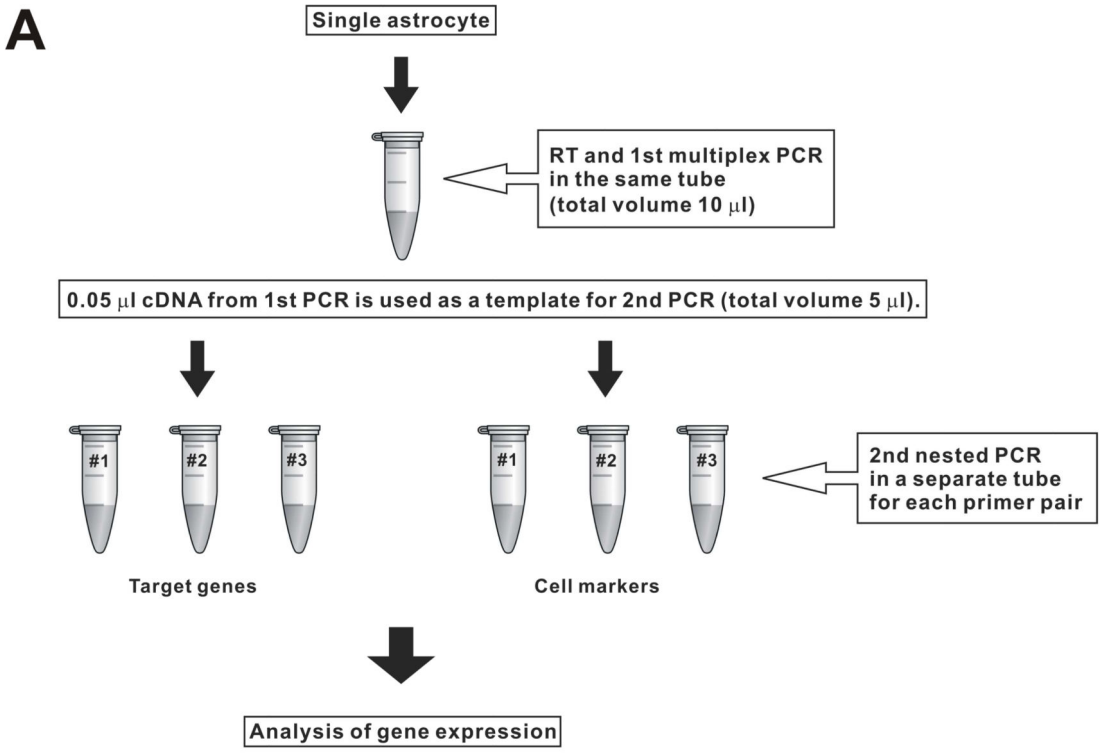

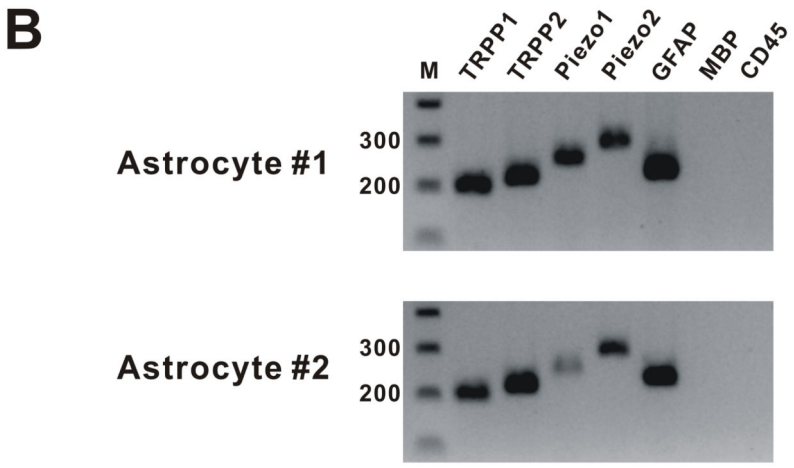

Fig. 3.

Single-cell gene expression analysis by reverse transcription PCR. **A.** Flow diagram of single-cell RT-PCR for a single optic nerve head astrocyte. **B.** Representative 2% agarose gels show that both astrocytes from the optic nerve head of GFAP-Cre × tdTomato mice express TRPP1-2 and Piezo1-2. GFAP, an astrocyte marker. MBP, an oligodendrocyte marker. CD45, a microglia marker. M, DNA length marker (100 bp ladder).

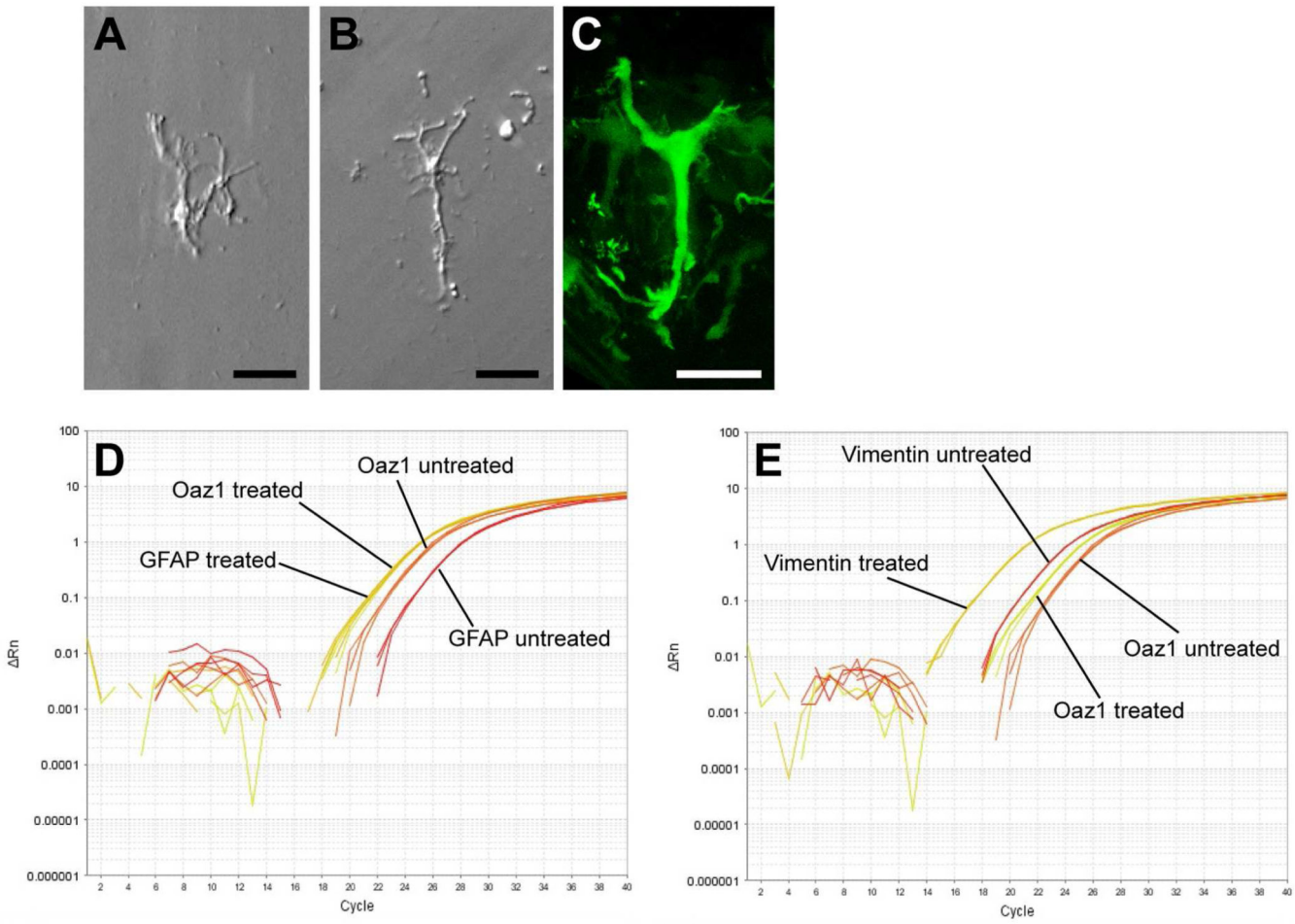

F C_T Value

	Untreated LE	Treated RE	Fold change ± SEM
GFAP	26.90 / 27.09 / 26.66 / 26.76	24.75 / 24.04 / 26.73 / 25.00	2.67 ± 0.67
Vimentin	20.98 / 23.29 / 22.45 / 22.81	19.96 / 20.28 / 22.16 / 20.45	2.68 ± 0.89

Fig. 4.

Quantitative PCR from 12 isolated astrocytes 1 day after optic nerve crush. **A-B.** Dissociated astrocytes from the crushed optic nerve have fewer and thicker processes than their uninjured counterparts. **C.** A typical astrocyte 1 day after optic nerve crush (agarose section from a B6.hGFAPpr-EGFP mouse) for comparison of the morphology. **D.** Amplification curves for the expression of the GFAP gene in the isolated astrocytes from contralateral untreated (left) versus crushed (right) optic nerves. **E.** Amplification curves for vimentin. **F.** C_T values for the 4 biological replicates are given for both genes. This would indicate a ~2.7–fold up-regulation (mean ± SEM) for GFAP and vimentin. All scale bars: 20 μm.